Physica Medica 114 (2023) 103158

Contents lists available at ScienceDirect

Physica Medica

journal homepage: www.elsevier.com/locate/ejmp

Original paper

Pilot scale validation campaign of gel dosimetry for pre-treatment quality assurance in stereotactic radiotherapy

G. Magugliani [a,*], M. Marranconi [b], G.M. Liosi [a], F. Locatelli [b], A. Gambirasio [b], L. Trombetta [b], V. Hertsyk [c], V. Torri [d], F. Galluccio [a], E. Macerata [a], E. Mossini [a], A. Santi [a], M. Mariani [a], E. Bombardieri [e], V. Vavassori [f], P. Salmoiraghi [b]

[a] Department of Energy, Nuclear Engineering Division, Politecnico di Milano, Milano, Italy
[b] U. O. Medical Physics, Humanitas Gavazzeni, Bergamo, Italy
[c] Fondazione Humanitas per la Ricerca, Milano, Italy
[d] Department of Oncologic Research, Istituto di Ricerche Farmacologiche Mario Negri IRCCS, Milano, Italy
[e] Scientific Direction, Humanitas Gavazzeni, Bergamo, Italy
[f] U. O. Radiotherapy, Humanitas Gavazzeni, Bergamo, Italy

ARTICLE INFO

Keywords:
Gel dosimetry
3D dosimetry
Pre-treatment dosimetry
Radiotherapy QA
Validation campaign
Stereotactic radiotherapy

ABSTRACT

Purpose: Complex stereotactic radiotherapy treatment plans require prior verification. A gel dosimetry system was developed and tested to serve as a high-resolution 3D dosimeter for Quality Assurance (QA) purposes.
Materials and Methods: A modified version of a polyacrylamide polymer gel dosimeter based on chemical response inhibition was employed. Different sample geometries (cuvettes and phantoms) were manufactured for calibration and QA acquisitions. Irradiations were performed with a Varian Trilogy linac, and analyses of irradiated gel dosimeters were performed via MRI with a 1.5 T Philips Achieva at 1 mm^3 or 2 mm^3 isotropic spatial resolution. To assess reliability of polymer gel data, 54 stereotactic clinical treatment plans were delivered both on dosimetric gel phantoms and on the Delta4 dosimeter. Results from the two devices were evaluated through a global gamma index over a range of acceptance criteria and compared with each other.
Results: A quantitative and tunable control of dosimetric gel response sensitivity was achieved through chemical inhibition. An optimized MRI analysis protocol allowed to acquire high resolution phantom dose data in timeframes of ≈ 1 h. Conversion of gel dosimeter data into absorbed dose was achieved through internal calibration. Polymer gel dosimeters (2 mm^3 resolution) and Delta4 presented an agreement within 4.8 % and 2.7 % at the 3 %/1 mm and 2 %/2 mm gamma criteria, respectively.
Conclusions: Gel dosimeters appear as promising tools for high resolution 3D QA. Added complexity of the gel dosimetry protocol may be justifiable in case of small target volumes and steep dose gradients.

1. Introduction

Nowadays Stereotactic Radiosurgery (SRS) and Stereotactic Body Radiation Therapy (SBRT) are common treatment approaches employed for cranial and extracranial targets [1,2]. Sharp collimation, small target volumes and high doses per fraction exploited by these techniques entail a careful dosimetric pre-treatment evaluation as part of the Patient-Specific Quality Assurance (PSQA) program. In several countries, this is also a legal requirement [3].

Experimental validation of calculated treatment plans can be performed by different technical means, with variable levels of complexity. The preferred approach should be based on a truly composite QA process [4], where the absorbed dose distribution is determined in a three dimensional phantom. Several dosimetric devices specifically developed for composite PSQA are nowadays available on the market [5–9]: these are typically constituted of two-dimensional arrays of radiation detectors such as diodes or small-volume ionization chambers. While presenting the advantages of active detectors, these are unable to perform a truly direct volumetric mapping of absorbed dose, being limited by their 2D configuration. Moreover, for small target sizes characteristic of stereotactic treatments, only a limited number of dose data points is typically collected by these devices due to their finite

* Corresponding author.
E-mail address: gabriele.magugliani@polimi.it (G. Magugliani).

https://doi.org/10.1016/j.ejmp.2023.103158
Received 19 April 2023; Received in revised form 25 September 2023; Accepted 28 September 2023
Available online 6 October 2023

spatial resolution and detector arrangement. This can be particularly problematic in penumbra regions, for which sharp dose gradients may be inadequately sampled [10].

In this context, the interest in gel dosimeters for QA purposes [11,12] is motivated by their tissue equivalency [13–16], and their intrinsic volumetric response which results in high – and isotropic – spatial resolution, also negating detector volume averaging effects [17].

Initial development of polymer gel dosimeters dates back to the nineties [18]. In the following decades, several formulations have been developed, employing different monomers and gelling matrices [19–25], some of which capable of simulating low density tissue [26–28], also in a combined manner [29]. Various additives have also been proposed to modify and stabilize the dose–response of polymer gel formulations [30,31], resulting in a very broad range of available compositions, each characterized by a different sensitivity and range of response.

Polymer gel dosimeters express a physical response in terms of induced polymerization between constituting monomers following irradiation [12,32]. Being the polymerization yield locally dependent on absorbed dose, phantoms prepared from such dosimetric gels can be considered as having an intrinsic and spatially stable 3D dose–response. Many imaging techniques can be adopted for the volumetric analysis of irradiated dosimetric gels, like ultrasound tomography [33], optical tomography [34] and X-Ray CT [35]. Since local polymerization directly influences ^{1}H nuclear spin relaxation, MRI is routinely used for the analysis of irradiated polymer gels [36,37]. Exploiting in particular the two latter techniques which allow immediate analysis following irradiation thanks to onboard imaging systems, recent applications of polymer gel dosimeters also regard evaluation of isocenter accuracy for MRI guided-LINACs [38,39] and verification of coincidence between radiation and onboard cone beam CT imaging systems [40,41].

When MRI is employed as the analysis technique, a T_2-weighted sequence is typically employed, allowing for 3D relaxation mapping and hence, after proper calibration, 3D dosimetry. Optimization of MRI analysis protocol plays a fundamental role in the overall reliability of polymer gel data. This often consists in a balancing act between achievable signal noise and required acquisition time [42].

Several drawbacks however still hinder a widespread adoption of these specialized devices. To begin with, as for any passive dosimeter, the range of response of gels dosimeters is in general not matched to the dose range of interest of the specific acquisition in which they are employed. This can result in only partial use of their response range or, at the opposite, in the need of down-scaling of planned doses in order to avoid response saturation. This latter approach is not without drawbacks, since it can impose augmented mechanical stresses and accelerations in linac components, thus possibly altering the representativeness of the QA process [43]. To overcome such limitations different dosimetric gel compositions with proper ranges of response can be used depending on the case being considered. This strategy is however not ideal, as it may require the development of several preparation-analysis protocols, as well as the need to acquire many types of monomers and additives. In this study, a modified version of the acrylamide-based normoxic polymer gel dosimeter PAGAT was used [44,45]. The addition of the polymerization inhibitor p–nitrophenol was investigated as a simple and effective means of quantitatively controlling the sensitivity – and hence the range of response, dose resolution and minimum detectable dose [45–47] – of the dosimetric gel. The advantage of this approach consists in allowing optimal tailoring dosimeter response to the dose range of interest for each specific pre-treatment evaluation, without the need of significantly altering the composition of the dosimetric gel or requiring adaptations in its manufacturing protocol.

Another known weakness of gel dosimetry consists in the difficulty in performing quantitative dose evaluations due to dependence of polymer gel response upon phantom geometry and manufacturing batch [48,49], which results in a lack of generalized reproducibility. Several strategies have been proposed in literature to allow the reliable determination of absorbed dose, such as rescaling on independent pointwise dose measurements provided by TLDs [50] or active detectors [51], or the adoption of some kind of normalization to a known reference response [52,53]. In this work, an internal calibration protocol was developed to this scope. This approach is further described in section 2.3 and is based on an extrapolation of sensitivity from calibration samples and subsequent normalization to individual phantom response.

The purpose of this research consisted firstly in the definition of a 3D dosimetric protocol based on variable-sensitivity polymer gel dosimeters to be employed in PSQA. The results of a pilot scale testing of reliability and robustness was then performed through pre-treatment acquisitions of 54 actual SRS/SBRT treatment plans.

2. Materials and Methods

2.1. Polymer gel dosimeter preparation

The overall composition of dosimetric gels employed in this work is reported in Table 1 [45]. All reagents used for their synthesis were of analytical grade and were purchased from Merck KGaA. To manufacture a batch of dosimetric gel, acrylamide and N,N'-methylenebisacryamide monomers are firstly dissolved in deionized water under stirring at 50 °C. Concurrently, a gelatin (from porcine skin, Type A) solution is prepared in an identical way in the remainder of the overall water volume. Once both the monomers and the gel solutions have cooled below 30 °C, they are mixed together. Depending on the desired dose range of response and sensitivity for the polymer gel batch under production, the appropriate quantity of p-nitrophenol inhibitor is then added [45], followed by tetrakis(hydroxymethyl)phosphonium chloride (THPC). The dosimetric solution can then be poured in the desired container which is stored under refrigeration at 4 °C for at least 12 h and for a maximum of 36 h before irradiation. Prepared dosimetric gels were slightly opaque and did not show presence of suspended matter or precipitates. Variable levels of inhibition were tested as reported in Table 1, in order to determine its effect on sensitivity of dose range of linearity of the resulting formulation.

Two types of sample geometries were prepared: spectrophotometric PMMA cuvettes (1 mm wall thickness, Kartell S.p.A.) and 500 ml HDPE cylindrical bottle phantoms (1 mm wall thickness, DWK Life Sciences Ltd.). The former were employed to perform dose–response characterizations (evaluation of linearity, range of response, accuracy/precision, etc. as reported in section 3.1) via irradiation at known uniform doses. The latter were instead used for volumetric acquisitions and pre-treatment evaluations. Typically, up to 4 phantoms and one set of cuvette samples were prepared from a single batch of dosimetric gel.

2.2. Irradiation and MRI analysis

A Trilogy linac (Varian Medical Systems, Inc) was used for all irradiations performed in this work, exclusively employing a 6 MV acceleration energy (WFF beams). Variable dose rates in the range 100 – 1000 MU min^{-1} (corresponding to 1.0 – 10.4 Gy min^{-1} in the adopted cuvette irradiation setup as reported in Fig. 1a) were investigated during characterization of gel dosimeter formulation to assess possible dependencies of dose response with respect to this parameter. The

Table 1
Composition of dosimetric gels. Inhibitor concentration was selected in the reported range according to the desired sensitivity.

Reagent	Concentration
Gelatin	5 wt%
Acrylamide	3 wt%
N,N'-methylenebisacryamide	3 wt%
THPC	10 mM
p-nitrophenol	5 – 20 ppm

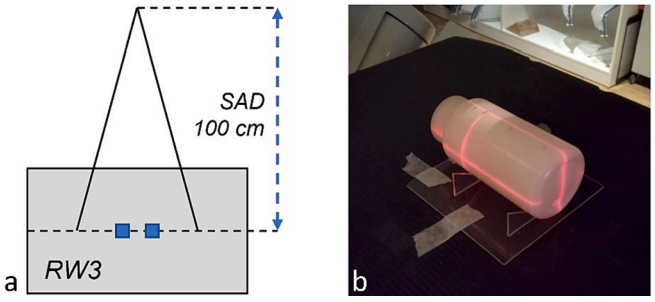

Fig. 1. a) positioning of cuvettes in RW3 slab phantom with indication of the adopted source-axis-distance (SAD). b) dosimetric phantoms positioned on dedicated holder.

treatment planning system in use was Varian Eclipse (v. 15.5, employing AAA v. 5.5.12), with an isotropic dose grid size of 1 mm^3.

Cuvette samples of dosimetric gel employed for characterization were positioned in a RW3 slab phantom (PTW Freiburg GmbH, Fig. 1a) in order to achieve as high as possible dose uniformity in their sensitive volume. Preliminary CT imaging and TPS calculation performed on this irradiation setup confirmed a dose uniformity > 99 % when two antero-posterior and postero-anterior fields (20 cm × 30 cm) were used. Typical reproducibility in delivered dose for static open field irradiations as those employed for gel dosimeter response characterization were within 1 % and were therefore considered negligible. Volumetric polymer gel phantoms were instead immobilized on the treatment couch via a dedicated holder which guaranteed high positioning reproducibility, as illustrated in Fig. 1b. Also in this case, CT imaging was employed to acquire the geometric dataset necessary for TPS planning on phantom geometry. All dosimetric samples were allowed to thermalize before undergoing irradiation and were subsequently stored under refrigeration for 24 h before proceeding to MRI analysis to allow for the full development of their chemical response.

T_2-weighed MRI analyses of dosimetric gels were performed with a Philips Achieva D-Stream 1.5 T, equipped with an 8 ch. Sense NV head & neck receiver coil. Up to 4 phantoms could be scanned simultaneously with this setup. Complete thermalization of gel dosimeter cuvettes and phantoms was achieved prior to their MRI analysis. A gradient spin echo sequence – available by default on the scanner – was employed (TR = 5 s, TE = 40 ms, 14 echoes, TSE = 14, EPI = 5, 6 signal acquisition averages), as this represented an ideal compromise between acquisition time and resulting signal noise (see also supplementary materials file). An isotropic spatial resolution of 1 mm^3 was adopted for signal acquisitions. It is known that the performance of the dosimetric system as a whole is indeed dependent not only on the physico-chemical dose response of the dosimetric gel, but also on its accompanying MRI protocol [42]. The adopted spatial resolution directly affects the noise of MR images and, hence, of dosimetric data. To investigate quantitatively how acquisition resolution affects dosimeter performance and agreement with the Delta4 reference dosimetric system, raw polymer gel phantom MRI data was also rescaled from the native 1 mm^3 resolution up to 2 mm^3 isotropic through linear averaging. This post-acquisition rescaling can be considered, with good approximation, as equivalent to a direct MRI analysis with the same 2 mm^3 voxel size, since this imaging technique naturally performs an average of proton relaxation over the volume of each voxel.

R_2 values were determined on a voxel-by-voxel basis via interpolation of signal intensity with the appropriate Bloch function [42] through a dedicated algorithm specifically developed in the Matlab environment.

In the case of calibration specimens, average spin–spin relaxation rate values $R_2 = 1/T_2$ were put in correspondence with absorbed dose in D-R_2 plots. Dose conversion of acquired R_2 distributions for volumetric phantoms was instead performed according to the internal calibration procedure described in the following section.

In all reported graphs, error bars represent one standard deviation of uncertainty.

2.3. Internal calibration

Sensitivity S_j of a specific batch of dosimetric gel j was defined as the slope of the linear regression in a D-R_2 plot as determined via same-batch cuvette samples. Experimental evidence, as will be presented in the following sections, indicated that the value of S_j remained constant among all samples from the same polymer gel batch, regardless of their geometry. The value of batch-specific sensitivity S_j was therefore employed for the dose conversion of relaxation data $R_{2,ij}$ of *i-th* phantom of the *j-th* batch considering the following D-R_2 linear relationship [45]:

$$R_{2,ij} = \left(S_j D + b_j\right) + \delta_i$$

where δ_i essentially represents a phantom-specific difference in R_2 blank value with respect to that of corresponding cuvettes b_j – also indicated in the following as "shift factor". Graphically, this is identifiable as the rigid shift between dose response curves (see also Fig. 4). The origin of this shift is attributable to different thermal histories among samples, in part also deriving from decreased cooling rates for large volume phantoms when compared to cuvettes adopted for calibration [48,54].

Shift factors for each phantom were determined by scanning a non-irradiated portion of their volume concurrently with volumetric data mapping in the region employed for plan dosimetry. This internal calibration procedure relies both on linearity of response of the dosimetric gel and the invariance of response sensitivity among different container shapes of the same dosimetric gel batch (cuvettes *vs* phantoms). The former aspect was verified for each preparation batch, as described in the following section. Invariance of sensitivity among different sample geometries was verified by comparing the D-R_2 response between cuvettes and several volumetric phantoms irradiated at the same dose, over their corresponding linearity range. A behavior compatible with invariance of response, except for a different blank level accounted for via the shift factor, was noted across different batches of dosimetric gel, also employing variable inhibition levels.

2.4. Pre-treatment measurements and reference dosimetry

To assess the reliability of gel dosimetry, 54 treatment plans were identified (anatomical targets: 23 brain, 3 lymph nodes and 28 lungs, average PTV volumes 4.4, 10.8 and 12.3 cm^3 respectively) upon which pre-treatment evaluations were performed. Maximum planned doses (D_{max}) in coplanar geometry[1] were in the range 9.3 – 30 Gy. These plans were delivered on dosimetric gel phantoms specifically manufactured with a level of inhibition resulting in the highest dosimetric gel sensitivity compatible with the maximum dose D_{max} to be expected for each plan. Since D_{max} were determined from TPS calculations, the adopted level of inhibition also accounted for possible uncertainties in these values in order to avoid exceeding the response linearity range of the dosimetric gel. Namely, this was assessed by means of a set of calibration cuvettes for each batch of dosimetric gel up to a level corresponding to 110 % of D_{max}. As described in the previous paragraph, the use of calibration cuvettes was also necessary to allow the conversion of phantom R_2 data to absorbed dose values. When multiple plans shared a similar maximum dose, a corresponding number of phantoms could be prepared from the same batch of dosimetric gel, thus requiring the use of only a single set of calibration cuvettes.

The validation of PSQA results obtained by dosimetric gels should rely on their comparison with equivalent data, which can be deemed reliable. The Delta4 dosimetric system was employed as a reference

[1] As explained later in this section, D_{max} was evaluated in such geometry due to constraints in the adopted validation protocol.

measurement device for this scope. This instrument is constituted by a cylindrical water equivalent body in which two planar orthogonal arrays of p-Si detectors are embedded. The pitch between detectors in the central area (6 cm × 6 cm) is 5 mm, while in the periphery (20 cm × 20 cm) it is 10 mm. The 54 treatment plans were therefore delivered identically on both dosimetric gel phantoms and on this reference dosimetric system. To satisfy restrictions imposed by the Delta4, all irradiations were performed in coplanar geometry with couch at 0° position, even if they were originally defined in a non-coplanar way. For consistency, as mentioned before, also all dosimetric gel phantoms were therefore irradiated in the same coplanar geometry.

A direct comparison between dose measurements from Delta4 and dosimetric gel phantoms is not possible due to the different geometry of the two devices. An *indirect* validation of dosimetric data was therefore performed by comparing each experimental measurement provided by the two devices with its coupled TPS calculation (implemented in the corresponding geometry) through a global gamma metric [55]. These separate gamma evaluations were then compared together to assess the discrepancy between the results obtained from dosimetric gels and Delta4 in terms of agreement with respective TPS data for all 54 treatment plans considered.

A 3D global gamma index (10 % absolute dose threshold) was employed as the dose comparison criterion between measured and calculated dose data, *i.e.* dosimetric gel *vs* TPS and, separately, Delta4 *vs* TPS. A range of distance to agreement (DTA: from 1 mm to 5 mm, 0.5 mm increments) and dose difference (DD: from 1 % to 5 %, 0.5 % increments) were considered, in order to more comprehensively represent the agreement between each of the two instruments with corresponding TPS calculations and, indirectly, the agreement between devices themselves.

3. Results

3.1. Characterization of gel dosimeter formulation

Irradiation and MRI analysis of cuvette groups prepared with variable inhibitor content as specified in Table 1 allowed to determine relationships between p-nitrophenol concentration and resulting D-R_2 sensitivity and range of linear response. Fig. 2a reports correlations between these quantities as determined from such characterization campaign. The range of linearity was defined as the maximum dose range for which a corresponding D-R_2 coefficient of determination $R^2 >$ 0.98 was recorded. As evident from the graph, an inverse relationship between sensitivity and linearity range was noted, coherently to the inhibitory effect expressed by p-nitrophenol [45]. The typical reproducibility of dosimetric performance across different dosimetric gel batches was ≈ 10 %.

The dependence of dosimetric gel response on dose rate was tested with irradiation at fixed doses (5–10-15 Gy) and variable dose rate in the range available from the linac (100 – 1000 MU min^{-1}). To achieve comparable beam-on irradiation time among all samples, proper waiting periods were introduced for higher dose rate irradiations. This step was necessary in order to compensate for the known gel dosimeter response dependence upon irradiation length [56,57]. As reported in Fig. 2b, a very significant variability of response was noted for lower dose rates. This however decreases to < 1 % in the range 600 – 1000 MU min^{-1}, *i.e.* the rate typically employed for SRS/SBRT irradiations, irrespectively from total dose. No significant effect of inhibitor content was noted on the dose rate response of the gel dosimeter formulation. Additional data concerning the characterization of dosimetric formulations with variable inhibition levels is provided in a supplementary materials file.

3.2. Dose response of volumetric phantoms

The spatial resolving capabilities of a dosimetric gel phantom were tested via a half-closed field irradiation on a 360° arc, providing a very sharp dose gradient along its longitudinal axis, with uniform dose across its transverse sections. Fig. 3 reports a comparison between calculated and resulting measured relative axial dose profiles for a 26 Gy

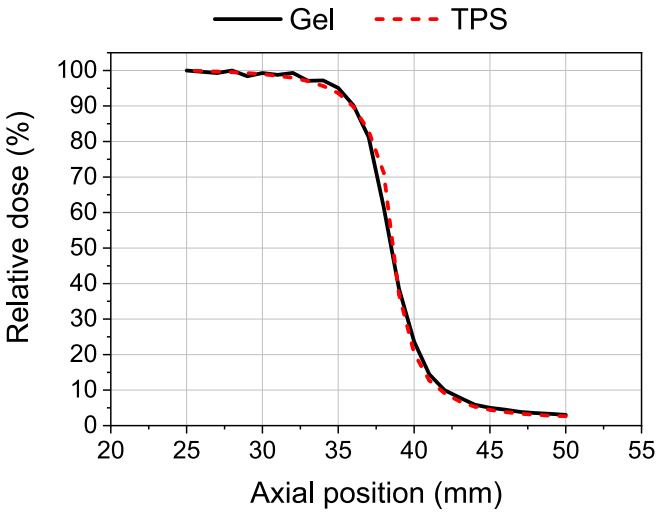

Fig. 3. Planned and measured axial dose profiles corresponding to a half-closed irradiation field. Maximum dose and dose gradient are 26 Gy and 10 Gy mm^{-1}, respectively. Uncertainty associated to gel dosimeter profile ≈ 2 %, not reported for clarity. Dosimetric gel formulation with 20 ppm p-nitrophenol.

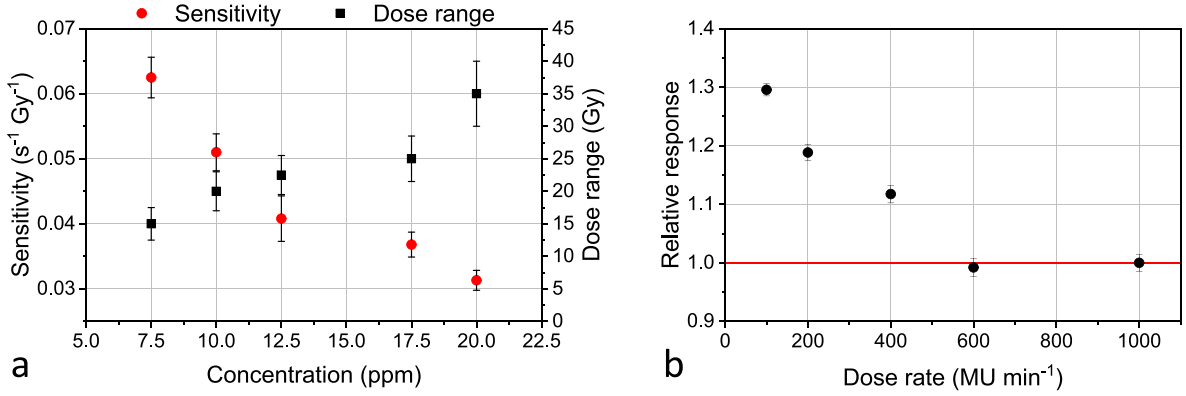

Fig. 2. a) dependence of response sensitivity and range of linear response with respect to p-nitrophenol inhibitor concentration (constant dose rate 600 MU min^{-1}). b) dependence of relative R_2 dosimetric gel response with respect to irradiation dose rate, normalized to the value obtained at 1000 MU min^{-1} (constant dose 10 Gy, 10 ppm p-nitrophenol).

irradiation of a 20 ppm p-nitrophenol formulation.

A 100 % gamma passing rate (1 %/1 mm) was recorded for the reported axial profile. Equivalent evaluations performed on the same phantom stored under refrigeration for 3 months after irradiation resulted in essentially identical dose profiles, showing the same gamma agreement. This indicates the absence of dose overshoot or diffusion phenomena, the two principal causes of response instability reported for gel dosimeters [58,59]. Also in this case, repetition of this investigation at different inhibition levels (7.5 and 12.5 ppm) resulted in the same conclusions.

As a final step in the characterization campaign, to study the dependence of batch-specific dose response upon sample geometry, *i.e.* cuvette *vs* phantom, volumetric phantoms were irradiated with uniform axial bands obtained by superimposing four orthogonal radial fields (0° – 90° – 180° – 270°) for each dose region. Fig. 4a illustrates an example of such irradiation pattern. Employed doses spanned the linearity range expected according to the adopted inhibition level. Axial separation between irradiation bands provided minimal cross-contamination between prescribed doses (< 1 % from TPS). A corresponding blank R_2 value was also measured prior to irradiation for each phantom. Average R_2 determined in each portion of interest of the phantom volume was then compared with cuvette response curves, as illustrated in Fig. 4b. Such investigations were repeated across several preparation batches, also employing variable inhibition levels. Results indicated, among samples from the same batch of dosimetric gel *j*, invariance of sensitivity S_j (variability within uncertainty of MRI analysis, typical ≈ 1.5 %) with however significant variability in blank values across phantoms, as further described in the following paragraph.

3.3. Pre-treatment acquisitions

Each of the 54 treatment plans was irradiated on a dedicated gel dosimeter phantom which, as explained earlier, was manufactured with a level of inhibition adapted to the maximum expected plan dose. A group of cuvettes was also prepared from each batch of dosimetric gel in order to determine its specific sensitivity S_j.

Reproducibility [37] of phantom blank R_2 values amounted to approximately 50 % and 150 % intra- and inter-batch, respectively. Accordingly, shift factors presented a similar dispersion and thus needed to be determined on a case-by-case basis through scanning of a non-irradiated portion of each phantom and subsequent comparison with calibration data from corresponding cuvette samples, as described in section 2.3.

After dose conversion via internal calibration, both dosimetric systems, *i.e.* gel dosimeter phantoms and Delta4, produced tables of gamma value with 81 entries for each of the 54 considered treatment plans. Every cell stores a value of gamma function corresponding to a combination of DD/DTA criteria. An example of such data is reported in Fig. 5 and in the supplementary materials file.

Agreement between corresponding values in the two tables was considered indicative of good reliability of gel dosimeter data, since the Delta4 was adopted as a gold standard. As expected, stricter DD/DTA criteria resulted in higher discrepancies between dosimetric gels and Delta4.

4. Discussion

With respect to other polymer gel formulations described in literature, the modified gel dosimeter composition as reported in this work presents the advantage of a controllable response without the need of modifying the type and concentration of monomers or the manufacturing protocol. Instead, only minor variations of inhibitor content are sufficient to obtain reproducible and quantitative control of dose response, achieving maximum sensitivity and dose resolution while maintaining a linear dose response compatible with the expected maximum plan dose. Maximization of dose sensitivity and resolution is crucial in order to exploit the full potential of the dosimetric system by optimally coupling it to the dose range of interest, and allowing to achieve the lowest minimum detectable doses [47].

The presented dosimetric gel composition exhibited a typical accuracy and precision of 2 %. As expected, these are strongly influenced by the MRI analysis protocol adopted. In general, longer analyses with multiple repetitions result in lowered signal noise, and hence improved precision. Tradeoffs must however be imposed with respect to total analysis time. The adopted sequence resulted in imaging time of ≈ 1 h for a dosimetric phantom, with the possibility of scanning up to 4 phantoms simultaneously (see also supplementary materials file).

Variability of gel dosimeter response outside the 600 – 1000 MU min^{-1} dose rate range as reported in Fig. 2 could result in dose overestimation. This can restrict the applicability of the proposed dosimetric gel formulation to QA scenarios in which only high dose rates – or a single fixed dose rate – is employed for the whole irradiation. This can be considered a limitation of the proposed dosimetric system since it hinders its general application in continuously variable dose rate conditions. For the SRS/SBRT plans considered in this study however, this did not represent a problem, since planned and actual delivery dose rates were always close to 1000 MU min^{-1}.

Comprehensive characterization of inhibitor effect allowed for an

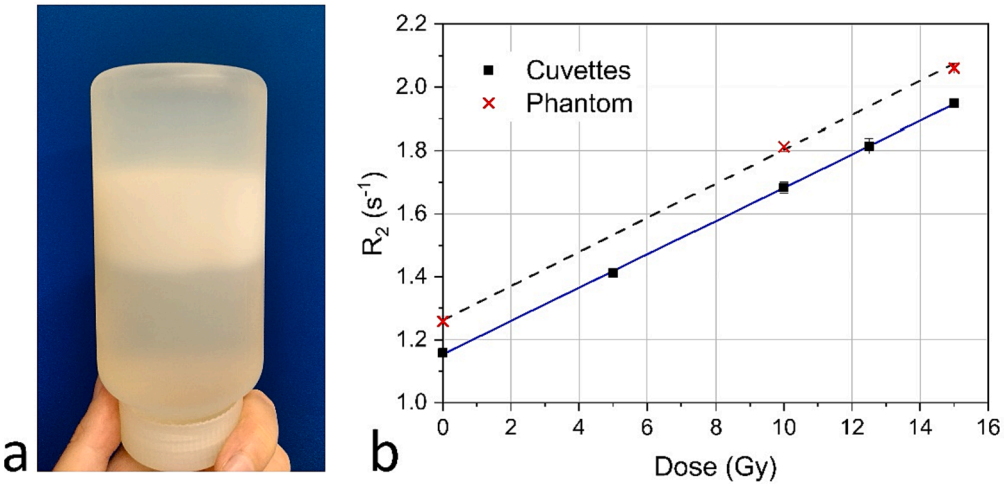

Fig. 4. a) example of phantom irradiated with a uniform axial dose band; b) comparison between dose response measured from a group of cuvettes and a volumetric phantom originating from the same batch of dosimetric gel. Sensitivity for both geometries is within the margin of uncertainty arising from MRI acquisitions.

DTA (mm) \ DD (%)	1	1,5	2	2,5	3	3,5	4	4,5	5
5	100	100	100	100	100	100	100	100	100
4,5	100	100	100	100	100	100	100	100	100
4	100	100	100	100	100	100	100	100	100
3,5	100	100	100	100	100	100	100	100	100
3	100	100	100	100	100	100	100	100	100
2,5	99,5	99,5	99,5	100	100	100	100	100	100
2	98,1	99	99,5	100	100	100	100	100	100
1,5	93,7	97,1	97,6	99	99,5	99,5	99,5	100	100
1	89,8	92,7	93,2	94,2	96,6	96,6	96,6	96,6	96,6

DTA (mm) \ DD (%)	1	1,5	2	2,5	3	3,5	4	4,5	5
5	99,9	99,9	100,0	100,0	100,0	100,0	100,0	100,0	100,0
4,5	99,8	99,9	99,9	99,9	99,9	100,0	100,0	100,0	100,0
4	99,5	99,7	99,8	99,9	99,9	99,9	99,9	99,9	100,0
3,5	98,9	99,3	99,6	99,7	99,8	99,8	99,9	99,9	99,9
3	96,8	97,9	98,5	99,0	99,3	99,5	99,7	99,8	99,9
2,5	94,9	96,5	97,5	98,2	98,7	99,1	99,4	99,6	99,7
2	88,4	91,0	92,9	94,5	96,0	97,2	98,0	98,6	99,1
1,5	82,6	86,4	88,9	91,0	92,5	93,7	95,2	96,5	97,5
1	61,4	66,5	71,1	75,2	79,3	82,9	85,8	88,2	90,8

Fig. 5. Gamma tables as obtained by Delta4 (left) and dosimetric gel phantom with 1 mm^3 isotropic resolution (right) for a brain target (PTV 4.7 cm^3, D_{max} 22 Gy). Passing rates < 90 % are highlighted in red. Global 3D gamma, 10 % absolute threshold.

easy identification of optimal inhibitor concentration for each preparation batch, according to data reported in Fig. 2. Optimal Inhibitor concentration could be reliably determined prior to irradiation only based on maximum planned dose D_{max}. For all tested plans, discrepancies between D_{max} and its experimental counterpart determined by the Delta4 were lower than 5 %. Concurrently, none of the 54 dosimetric gel phantoms exceeded their linearity range.

The very high spatial and temporal stability of dose profiles measured via phantoms drastically improves the robustness of the dosimetric system, especially against unforeseen analysis delays. This stability contrasts with literature results obtained for similar gel dosimeter formulations and may be attributed to a positive effect of the present inhibitor [37]. This however is currently only a speculation, to be confirmed by dedicated studies.

For a fixed composition, a typical reproducibility of batch specific sensitivity S_j across different preparations was ≈ 10 %. This value does not allow for a unique calibration of dosimetric gel response since it would result in unacceptable variability in QA data across different batches of dosimetric gel. However, a batch-by-batch dose response characterization can solve this limitation. The proposed internal calibration protocol appears adequate in allowing for absorbed dose evaluations, also accounting for variable phantom blank values. Compensation of intra-batch variability can be performed via the use of dedicated calibration samples used to determine the value of S_j. Differences in sensitivity between samples of the same batch and S_j as determined from related calibration cuvettes could be estimated as < 1.5 %, of the same magnitude of the precision of MRI acquisitions.

On the positive side, this internal calibration approach allows for the simultaneous preparation and subsequent analysis of multiple phantoms. This improves the logistical appeal of the dosimetric system, and partly compensates for the added time required for the irradiation of the cuvette group necessary to determine the batch-specific sensitivity S_j.

4.1. Reliability of gel dosimetry based PSQA and effect of spatial resolution

An isolated evaluation of gel dosimeter *vs* TPS passing rates is not adequate in declaring reliability of dosimetric data, since, by the intrinsic nature of PSQA, it is not possible to know a priori that plan irradiation will fully comply to TPS calculation. The comparison of gamma analysis results from two devices, *i.e.* Delta4 and gel dosimeters, is instead a better metric of performance and reliability.

Fig. 6 reports a summary of the absolute value-difference between gamma passing rate values determined via Delta4 and dosimetric gel phantoms averaged over the 54 plans considered. Both native 1 mm^3 and rescaled 2 mm^3 resolutions are reported. A significant improvement in terms of agreement between the two devices can be noted as the voxel size for dosimetric gel phantoms is increased from 1 to 2 mm^3.

Average gel dosimeter-Delta4 gamma discrepancies for the two criteria of clinical interest of 3 %/1 mm and 2 %/2 mm, amounted to 4.8 % – 10.8 % and 2.7 % – 5.8 % for 2 mm^3 and 1 mm^3 resolution, respectively. The most relevant enhancement of the agreement was scored for the stricter DD/DTA combinations. Such improvements underline how the reliability of dosimetric gel data for very small voxel sizes is likely limited by the image quality achievable by MRI analysis, rather than intrinsic limitations of the gel dosimeter formulation. In fact, for gel dosimeters the adoption of a specific analysis resolution also dictates the effective "gel detector" size, *i.e.* the voxel. Hence, a coarser resolution provides for lower signal noise associated to each voxel, better data accuracy, and therefore a higher gamma agreement. This is in contrast to what may be expected for active array detectors, for which a higher resolution is expected to result in better gamma passing rates since in this case accuracy of dose data is not dominated by detector noise [60].

Fig. 7 reports Bland-Altman plots for the 3 %/1 mm and 2 %/2 mm criteria (2 mm^3 dosimetric gel resolution). A slight but systematic

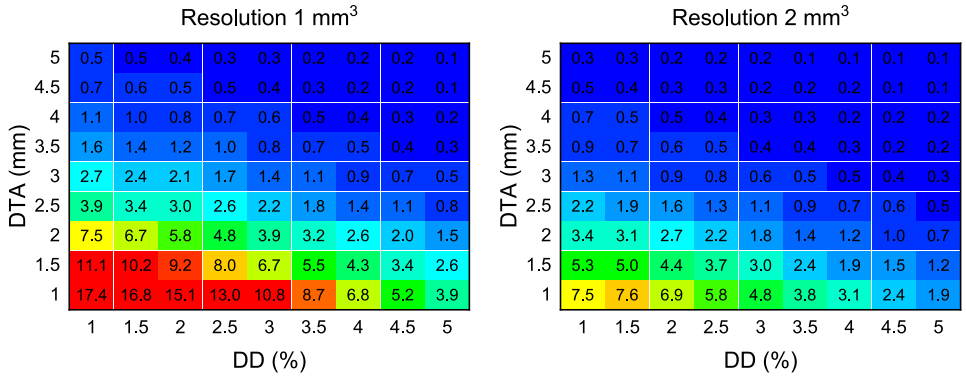

Fig. 6. Absolute difference between global gamma passing rate values measured by dosimetric gel phantoms and Delta4 averaged over the 54 treatment plans, according to the considered DD/DTA criteria. Spatial resolution of gel dosimeter data of 1 mm^3 (left) or 2 mm^3 (right). Color scale qualitatively indicates the absolute magnitude of average passing rate difference.

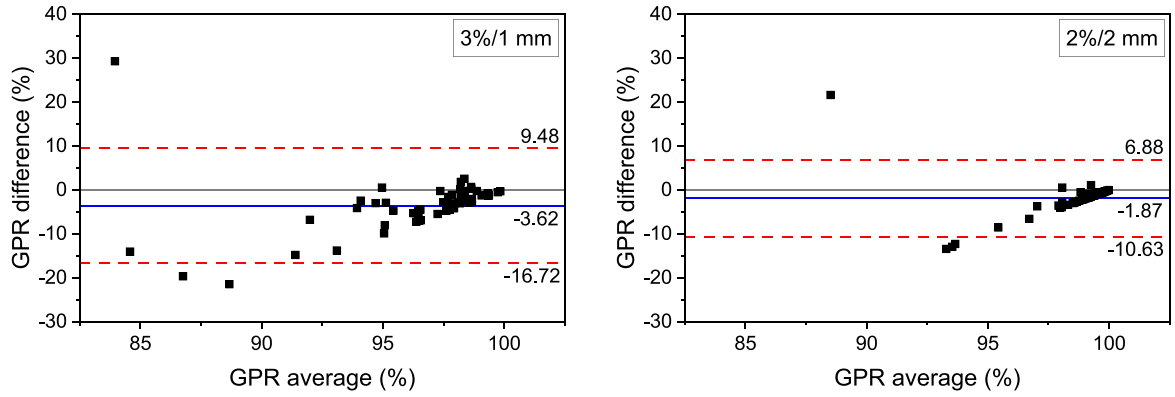

Fig. 7. Bland-Altman plots constructed from the difference between gamma passing rates (GPR) measured by Delta4 and dosimetric gels (2 mm^3 resolution) for 3 %/1 mm and 2 %/2 mm criteria. Average difference and 95 % limits of agreement indicated by solid blue and red dashed lines, respectively.

underestimation of gamma passing rate by gel dosimeters can be noted in both cases, which is less pronounced for the latter criteria. Considering only passing rates > 97.5 %, the differences between the two devices are instead very limited, and indeed for the 3 %/1 mm criteria ≈ 10 % of plans presented a higher passing rate when analyzed with dosimetric gels. However, when all plans are considered, a negative proportional bias can be noted.

Table 2 reports a comparison of the number of treatment plans which satisfy two common gamma criteria thresholds (minimum 90 % passing rate at 3 %/1 mm and 2 %/2 mm). Evaluations from dosimetric gel phantoms at 2 mm^3 isotropic resolution returned similar results as the Delta4. A significantly lower fraction of plans satisfies the QA threshold for the finer 1 mm^3 resolution, especially for the 3 %/1 mm criteria.

This type of comparison, being purely categorical, does not quantify the agreement between devices as is instead presented in the previous paragraphs and illustrated in Fig. 6 and Fig. 7. It is nonetheless useful in highlighting how the acceptability of a treatment plan might vary depending on the instrument adopted for its evaluation. Since in this study the Delta4 was assumed as reference device, the high-resolution 1 mm^3 analysis protocol results in an unjustified rejection of some treatment plans attributable to a lesser performance of the gel dosimetric system. On the other hand, if analysis resolution is increased to 2 mm^3, gel dosimeter based PSQA would result in very similar plan acceptance as in the case of Delta4 use, thus suggesting a good robustness of the technique.

5. Conclusions

Addition of p-nitrophenol inhibitor to the PAGAT polymer gel dosimeter can be used to quantitatively control their dose response in a straightforward way. Highest sensitivity and lowest minimum detectable doses can thus be achieved by adapting the response of the dosimetric gel to each specific QA evaluation needs. When employed for PSQA of stereotactic treatment plans, gel dosimetry provides results comparable to that of Delta4. A slight but significant systematic underestimation of gamma passing rates from dosimetric gels is noted, which however only marginally affects the portion of plans not satisfying the minimum acceptance threshold. Accuracy of absolute dose data from polymer gels is strongly affected by the noise level in the adopted imaging technique, which limits the achievable spatial resolution.

As a final remark, it can be underlined that an improved validation protocol may be adopted to confirm the reliability of dosimetric gel data, also considering that the Delta4 is not specifically dedicated to SRS/SBRT dosimetry. To this scope, the fabrication of a tissue equivalent radiochromic film holder of the same geometry as dosimetric gel phantoms should be considered. This would allow a truly direct and fully rigorous comparison between experimental measurements provided by two independent devices.

Table 2
Number of plans achieving at least 90 % gamma passing rate for different DD/DTA criteria scored by Delta4 and dosimetric gel phantoms. Both 1 mm^3 and 2 mm^3 spatial resolutions are reported.

DD/DTA	Delta4	Polymer gel dosimeter	
		Resolution 1 mm^3	Resolution 2 mm^3
3 %/1 mm	53	23	50
2 %/2 mm	53	48	52

Declaration of Competing Interest

The authors declare that they have no known competing financial interests or personal relationships that could have appeared to influence the work reported in this paper.

Acknowledgment

The authors acknowledge the financial support granted by “5x1000 grant by Fondazione Humanitas per la Ricerca”.

Appendix A. Supplementary data

Supplementary data to this article can be found online at https://doi.org/10.1016/j.ejmp.2023.103158.

References

[1] Nieder C, Grosu AL, Gaspar LE. Stereotactic radiosurgery (SRS) for brain metastases: A systematic review. Radiat Oncol 2014;9:1–9. https://doi.org/10.1186/1748-717X-9-155.
[2] Wulf J, Hädinger U, Oppitz U, Thiele W, Ness-Dourdoumas R, Flentje M. Stereotactic radiotherapy of targets in the lung and liver. Strahlentherapie Und Onkol 2001;177:645–55. https://doi.org/10.1007/PL00002379.
[3] EURATOM. Council Directive 2013/59. n.d.
[4] Miften M, Olch A, Mihailidis D, Moran J, Pawlicki T, Molineu A, et al. Tolerance limits and methodologies for IMRT measurement-based verification QA: Recommendations of AAPM Task Group No. 218. Med Phys 2018;45:e53–83. 10.1002/MP.12810.
[5] Stathakis S, Myers P, Esquivel C, Mavroidis P, Papanikolaou N. Characterization of a novel 2D array dosimeter for patient-specific quality assurance with volumetric arc therapy. Med Phys 2013;40(7):071731.
[6] Ĺtourneau D, Publicover J, Kozelka J, Moseley DJ, Jaffray DA. Novel dosimetric phantom for quality assurance of volumetric modulated arc therapy. Med Phys 2009;36:1813–21. https://doi.org/10.1118/1.3117563.
[7] Feygelman V, Forster K, Opp D, Nilsson G. Evaluation of a biplanar diode array dosimeter for quality assurance of step-and-shoot IMRT. J Appl Clin Med Phys 2009;10:64–78. https://doi.org/10.1120/JACMP.V10I4.3080.
[8] Padelli F, Aquino D, Fariselli L, De Martin E. IBA myQA SRS Detector for CyberKnife Robotic Radiosurgery Quality Assurance. Appl Sci 2022, Vol 12, Page 7791 2022;12:7791. 10.3390/APP12157791.

[9] James S, Al-Basheer A, Elder E, Huh C, Ackerman C, Barrett J, et al. Evaluation of commercial devices for patient specific QA of stereotactic radiotherapy plans. J Appl Clin Med Phys 2023;24(8). https://doi.org/10.1002/ACM2.14009.

[10] Taylor ML, Kron T, Franich RD. A contemporary review of stereotactic radiotherapy: Inherent dosimetric complexities and the potential for detriment. Http://DxDoiOrg/103109/0284186X2010551665 2011;50:483–508. https://doi.org/10.3109/0284186X.2010.551665.

[11] Papagiannis P, Karaiskos P, Kozicki M, Rosiak JM, Sakelliou L, Sandilos P, et al. Three-dimensional dose verification of the clinical application of gamma knife stereotactic radiosurgery using polymer gel and MRI. Phys Med Biol 2005;50(9): 1979–90.

[12] Baldock C, De Deene Y, Doran S, Ibbott G, Jirasek A, Lepage M, et al. Polymer gel dosimetry. Phys Med Biol 2010;55(5):R1–63.

[13] Taylor ML, Franich RD, Trapp JV, Johnston PN. Electron interaction with gel dosimeters: effective atomic numbers for collisional, radiative and total interaction processes. Radiat Res 2009;171:123–6. https://doi.org/10.1667/RR1438.1.

[14] Un A. Water and tissue equivalency of some gel dosimeters for photon energy absorption. Appl Radiat Isot 2013;82:258–63. https://doi.org/10.1016/J.APRADISO.2013.09.002.

[15] Pantelis E, Karlis AK, Kozicki M, Papagiannis P, Sakelliou L, Rosiak JM. Polymer gel water equivalence and relative energy response with emphasis on low photon energy dosimetry in brachytherapy. Phys Med Biol 2004;49:3495–514. https://doi.org/10.1088/0031-9155/49/15/013.

[16] Abtahi SMM, Bahrami F, Sardari D. An investigation into the dose rate and photon energy dependence of the GENA gel dosimeter in the MeV range. Phys Medica 2023;106:102522. https://doi.org/10.1016/J.EJMP.2022.102522.

[17] Trs-483, iaea.. Dosimetry of Small Static Fields Used in External Beam Radiotherapy. IAEA Tech Reports 2016. https://doi.org/10.1097/01.TP.0000149787.97288.A2.

[18] Maryanski MJ, Gore JC, Kennan RP, Schulz RJ. NMR relaxation enhancement in gels polymerized and cross-linked by ionizing radiation: A new approach to 3D dosimetry by MRI. Magn Reson Imaging 1993;11:253–8. https://doi.org/10.1016/0730-725X(93)90030-H.

[19] Kozicki M, Jaszczak M, Maras P, Dudek M. A chemical evolution of NVP-containing VIPAR-family 3D polymer gel dosimeters – a brief overview. J Phys Conf Ser 2019; 1305(1):012067.

[20] De Deene Y, Skyt PS, Hil R, Booth JT. FlexyDos3D: a deformable anthropomorphic 3D radiation dosimeter: radiation properties. Phys Med Biol 2015;60:1543–63. https://doi.org/10.1088/0031-9155/60/4/1543.

[21] Jaszczak M, Maras P, Kozicki M. Characterization of a new N-vinylpyrrolidone-containing polymer gel dosimeter with Pluronic F-127 gel matrix. Radiat Phys Chem 2020;177:109125. https://doi.org/10.1016/J.RADPHYSCHEM.2020.109125.

[22] Pappas E, Maris T, Angelopoulos A, Paparigopoulou M, Sakelliou L, Sandilos P, et al. A new polymer gel for magnetic resonance imaging (MRI) radiation dosimetry. Phys Med Biol 1999;44(10):2677–84.

[23] Schreiner LJ, Olding T, McAuley KB. Polymer gel dosimetry. J Phys Conf Ser 2010; 250:012014.

[24] Khan M, Heilemann G, Lechner W, Georg D, Berg AG. Basic Properties of a New Polymer Gel for 3D-Dosimetry at High Dose-Rates Typical for FFF Irradiation Based on Dithiothreitol and Methacrylic Acid (MAGADIT): Sensitivity, Range, Reproducibility, Accuracy, Dose Rate Effect and Impact of Oxygen Scavenger. Polymers (Basel) 2019;11. 10.3390/POLYM11101717.

[25] Senden RJ, De Jean P, McAuley KB, Schreiner LJ. Polymer gel dosimeters with reduced toxicity: a preliminary investigation of the NMR and optical dose–response using different monomers. Phys Med Biol 2006;51(14):3301–14.

[26] Gum F, Scherer J, Bogner L, Solleder M, Rhein B, Bock M. Preliminary study on the use of an inhomogenous anthropomorphic Fricke gel phantom and 3D magnetic resonance dosimetry for verification of IMRT treatment plans. Phys Med Biol 2002. https://doi.org/10.1088/0031-9155/47/7/401.

[27] Haraldsson P, Karlsson A, Wieslander E, Gustavsson H, Bäck SÅJ. Dose response evaluation of a low-density normoxic polymer gel dosimeter using MRI. Phys Med Biol 2006;51:919–28. https://doi.org/10.1088/0031-9155/51/4/011.

[28] De Deene Y, Vergote K, Claeys C, De Wagter C. Three dimensional radiation dosimetry in lung-equivalent regions by use of a radiation sensitive gel foam: proof of principle. Med Phys 2006;33:2586–97. https://doi.org/10.1118/1.2208939.

[29] Kozicki M, Bartosiak M, Maras P, Wach R, Kadlubowski S. First Combined, Double-Density LCV-Pluronic F-127 Radiochromic Dosimeter Mimicking Lungs and Muscles. Adv Mater Technol 2023;8:2201023. https://doi.org/10.1002/ADMT.202201023.

[30] Rabaeh KA, Al-Tarawneh RE, Eyadeh MM, Hammoudeh IME, Shatnawi MTM. Improved Dose Response of N-(hydroxymethyl)acrylamide Gel Dosimeter with Calcium Chloride for Radiotherapy. Gels 2022, Vol 8, Page 78 2022;8:78. 10.3390/GELS8020078.

[31] Kozicki M, Jaszczak M, Maras P, Dudek M, Cłapa M. On the development of a VIPARnd radiotherapy 3D polymer gel dosimeter. Phys Med Biol 2017;62(3): 986–1008.

[32] Kozicki M. How do monomeric components of a polymer gel dosimeter respond to ionising radiation: A steady-state radiolysis towards preparation of a 3D polymer gel dosimeter. Radiat Phys Chem 2011;80:1419–36. https://doi.org/10.1016/J.RADPHYSCHEM.2011.07.011.

[33] Mather ML, Baldock C. Ultrasound tomography imaging of radiation dose distributions in polymer gel dosimeters: Preliminary study. Med Phys 2003;30: 2140–8. https://doi.org/10.1118/1.1590751.

[34] Krstajić N, Doran SJ. Focusing optics of a parallel beam CCD optical tomography apparatus for 3D radiation gel dosimetry. Phys Med Biol 2006;51(8):2055–75.

[35] Jirasek A, Hilts M, McAuley KB. Polymer gel dosimeters with enhanced sensitivity for use in x-ray CT polymer gel dosimetry. Phys Med Biol 2010;55(18):5269–81.

[36] De Deene Y, Vandecasteele J. On the reliability of 3D gel dosimetry. J. Phys. Conf. Ser., 4714. 10.1088/1742-6596/444/1/012015.

[37] De Deene Y, Hanselaer P, De Wagter C, Achten E, De Neve W. An investigation of the chemical stability of a monomer/polymer gel dosimeter. Phys Med Biol 2000. https://doi.org/10.1088/0031-9155/45/4/304.

[38] Dorsch S, Mann P, Lang C, Haering P, Runz A, Karger CP. Feasibility of polymer gel-based measurements of radiation isocenter accuracy in magnetic fields. Phys Med Biol 2018;63:11NT02.;63(11):11NT02.

[39] Kim JH, Kim B, Shin W-G, Son J, Choi CH, Park JM, et al. 3D star shot analysis using MAGAT gel dosimeter for integrated imaging and radiation isocenter verification of MR-Linac system. J Appl Clin Med Phys 2022;23(6):e13615. https://doi.org/10.1002/ACM2.13615.

[40] Pant K, Umeh C, Oldham M, Floyd S, Giles W, Adamson J. Comprehensive radiation and imaging isocenter verification using NIPAM kV-CBCT dosimetry. Med Phys 2020;47:927–36. https://doi.org/10.1002/MP.14008.

[41] Adamson J, Carroll J, Trager M, Yoon SW, Kodra J, Maynard E, et al. Delivered Dose Distribution Visualized Directly With Onboard kV-CBCT: Proof of Principle. Int J Radiat Oncol Biol Phys 2019;103(5):1271–9.

[42] De Deene Y, Baldock C. Optimization of multiple spin-echo sequences for 3D polymer gel dosimetry. Phys Med Biol 2002. https://doi.org/10.1088/0031-9155/47/17/306.

[43] Park JM, Wu H-G, Kim JH, Carlson JNK, Kim K. The effect of MLC speed and acceleration on the plan delivery accuracy of VMAT. Br J Radiol 2015;88(1049): 20140698.

[44] Jirasek A, Hilts M, Shaw C, Baxter P. Investigation of tetrakis hydroxymethyl phosphonium chloride as an antioxidant for use in x-ray computed tomography polyacrylamide gel dosimetry. Phys Med Biol 2006;51(7):1891–906.

[45] Magugliani G, Liosi GM, Marranconi M, Micotti E, Caprioli M, Gambirasio A, et al. Practical role of polymerization inhibitors in polymer gel dosimeters. Nuovo Cim Della Soc Ital Di Fis C 2020;43. 10.1393/NCC/I2020-20147-7.

[46] De Deene Y, Van De Walle R, Achten E, De Wagter C. Mathematical analysis and experimental investigation of noise in quantitative magnetic resonance imaging applied in polymer gel dosimetry. Signal Process 1998;70:85–101. https://doi.org/10.1016/S0165-1684(98)00115-7.

[47] Piesch E, Burgkhardt B. Environmental monitoring. European interlaboratory test programme for integrating dosemeter systems 1984.

[48] Vandecasteele J, De Deene Y. On the validity of 3D polymer gel dosimetry: II. Physico-chemical effects Phys Med Biol 2013;58(1):43–61.

[49] De Deene Y. Gel dosimetry for the dose verification of Intensity Modulated Radiotherapy Treatments. Z Med Phys 2002;12:77–88. https://doi.org/10.1016/S0939-3889(15)70450-2.

[50] Mann P, Schwahofer A, Karger CP. Absolute dosimetry with polymer gels—a TLD reference system. Phys Med Biol 2019;64:045010. https://doi.org/10.1088/1361-6560/AAFD41.

[51] Pappas E, Maris TG, Zacharopoulou F, Papadakis A, Manolopoulos S, Green S, et al. Small SRS photon field profile dosimetry performed using a PinPoint air ion chamber, a diamond detector, a novel silicon-diode array (DOSI), and polymer gel dosimetry. Analysis and intercomparison Med Phys 2008;35(10):4640–8.

[52] Cardenas RL, Cheng KH, Verhey LJ, Xia P, Davis L, Cannona B. A self consistent normalized calibration protocol for three dimensional magnetic resonance gel dosimetry. Magn Reson Imaging 2002;20:667–79. https://doi.org/10.1016/S0730-725X(02)00596-9.

[53] Liney GP, Heathcote A, Jenner A, Turnbull LW, Beavis AW. Absolute radiation dose verification using magnetic resonance imaging: feasibility study. J Radiother Pract 2003;3:123–9. https://doi.org/10.1017/S1460396903000128.

[54] Deene YD, Pittomvils G, Visalatchi S. The influence of cooling rate on the accuracy of normoxic polymer gel dosimeters. Phys Med Biol 2007;52(10):2719–28.

[55] Low DA, Dempsey JF. Evaluation of the gamma dose distribution comparison method. Med Phys 2003;30(9):2455–64.

[56] Magugliani G, Liosi GM, Tagliabue D, Mossini E, Negrin M, Mariani M. Characterization of PAGAT dose response upon different irradiation conditions. Radiat Eff Defects Solids 2018. https://doi.org/10.1080/10420150.2018.1528604.

[57] Karlsson A, Gustavsson H, Månsson S, McAuley KB, Bäck SÅJ. Dose integration characteristics in normoxic polymer gel dosimetry investigated using sequential beam irradiation. Phys Med Biol 2007. https://doi.org/10.1088/0031-9155/52/15/021.

[58] De Deene Y, Venning A, Hurley C, Healy BJ, Baldock C. Dose-response stability and integrity of the dose distribution of various polymer gel dosimeters. Phys Med Biol 2002;47:2459–70. https://doi.org/10.1088/0031-9155/47/14/307.

[59] De Deene Y, Reynaert N, De Wagter C. On the accuracy of monomer/polymer gel dosimetry in the proximity of a high-dose-rate 192Ir source. Phys Med Biol 2001; 46:2801–25. https://doi.org/10.1088/0031-9155/46/11/304.

[60] Xia Y, Adamson J, Zlateva Y, Giles W. Application of TG-218 action limits to SRS and SBRT pre-treatment patient specific QA. J Radiosurgery SBRT 2020;7:135.